Q1: depence of particle radius. Q1-a: does model reproduce Fig.3 in Mason-Scheffold-2014? Most likely yes. Q1-b. Can the results on the depence on particle radius be physically explained?

Q2: dependence on temperature: model shows weak dependence on temperature. This is counter-intuitive. Can this be explained?

Kim and Mason's paper reproduction

Wei Fan

You can find the project code on GitHub: GitHub Repository.

Kim, Scheffold and Mason [2] developed a free energy model to describe the behavior of concentrated monodisperse emulsions, specifically focusing on systems with uniform droplet sizes that exhibit isotropic, disordered structures. This assumption of identical droplet sizes allows for a simplified and consistent analysis across different volume fractions, providing a clearer understanding of the emulsion properties. The model describes two key thermodynamic parameters: the osmotic pressure (Π) and the plateau storage modulus (G'_p), which reflects the linear elastic shear response. In such emulsions, based on the droplet volume fraction ϕ, three main contributions to the total free energy emerge: entropic, electrostatic, and interfacial forces. Each of these contributions dominates at different concentration ranges, leading to different responses in the behavior of the emulsion.

Q3: Kim-Mason makes no statements on the complex-value nature if the elastic modulus. Why? Does Kim-Mason predict the real part of the elastic modulus or the magnitude of the elastic modulus?

1 Free Energy

The free energy model uses the following parameters, the values of which were selected based on those provided in the original paper in order to be consistent with the system under study:

- $k_B = 1.38 \times 10^{-23}\,\mathrm{J/K}$ — Boltzmann constant
- $T = 298\,\mathrm{K}$ — Temperature in Kelvin
- $\sigma = 0.0098\,\mathrm{J/m^2}$ — Surface tension (converted from dyne/cm, this is a unit of surface tension in the CGS (centimeter-gram-second) system, where 1 dyne=10^{-5}N, 1 N/m = 1 J/m²)
- $a = 270 \times 10^{-9}\,\mathrm{m}$ — Droplet radius in meters
- $\xi = 0.15$ — Dimensionless parameter
- $\epsilon_r = 78.5$ — Relative permittivity of water
- $\epsilon_0 = 8.85 \times 10^{-12}\,\mathrm{F/m}$ — Permittivity of vacuum
- $\psi_0 = 270 \times 10^{-3}\,\mathrm{V}$ — Surface potential in volts
- $\lambda_D = 3.4 \times 10^{-9}\,\mathrm{m}$ — Debye length in meters
- $\phi_c = 0.646$ — Critical volume fraction
- $\alpha = 0.85$ — Shear effect parameter

The model consists of three core contributions to the total free energy:

- **Entropic term F_{ent}**: Represents the contribution of the entropy to the free energy of the emulsion system. Dominates at low volume fractions, where droplet interactions are minimal. Expressed as:

$$F_{\mathrm{ent}}(\phi, \phi_d)/N = -3k_BT \ln(\phi_c + \phi_d - \phi) \tag{1}$$

  where N is the number of droplets in the emulsion, T is the absolute temperature of the system, ϕ_c is the critical packing fraction, ϕ_d is the deformation volume fraction and k_B is the Boltzmann constant.

  Units Verification:

– *LHS:*

$$\frac{F_{\text{ent}}}{N} \quad (\text{Units: } \frac{\text{J}}{1} = \text{J})$$

– *RHS:*

$$-3k_BT\ln(\phi_c + \phi_d - \phi) \quad (\text{Units: } \frac{\text{J}}{\text{K}} \times \text{K} = \text{J})$$

The units on both sides of equation (1) are consistent, with both sides having units of energy (J).

- **Electrostatic term F_{elec}**: Represents the electrostatic interaction between charged droplet interfaces. Becomes prominent as the droplets approach closer to the jamming point $\phi_c \approx 0.646$, where screened electrostatic repulsions prevent further compression. Expressed as:

$$F_{\text{elec}}(\phi, \phi_d)/N = \frac{2\pi a^2 \epsilon_r \epsilon_0 \psi_0^2 \exp(-h/\lambda_D)}{h} \tag{2}$$

where a is the droplet radius, ψ_0 is the permittivity of vacuum, ϵ_r is the relative dielectric constant of the continuous phase, λ_D is the Debye screening length and h is the separation at the closest approach between the droplets, and is given by:

$$h(\phi, \phi_d) = 2\phi_c^{1/3} a \left[\phi^{-1/3} - \left(\phi_c + \phi_d - \alpha\gamma^2\right)^{-1/3}\right], \tag{3}$$

where γ is the applied shear strain, α is the dimensionless parameter representing the average shear effects on droplet configurations, accounting for non-affine local displacements during osmotic compression and shear.

Units Verification:

– *LHS:*

$$\frac{F_{\text{elec}}}{N} \quad (\text{Units: } \frac{\text{J}}{1} = \text{J})$$

– *RHS:*

$$\frac{2\pi a^2 \epsilon_r \epsilon_0 \psi_0^2 \exp(-h/\lambda_D)}{h} \quad (\text{Units: } \frac{\text{m}^2 \cdot \frac{\text{C}^2}{\text{N}\cdot\text{m}^2} \cdot \frac{\text{J}^2}{\text{C}^2}}{\text{m}} = \text{J})$$

The units on both sides of equation (2) are consistent, with both sides having units of energy (J).

- **Interfacial term**: Governs the system at higher volume fractions beyond ϕ_c, where increased droplet deformation is observed. Expressed as:

$$F_{\text{int}}(\phi_d)/N = 4\pi\xi\sigma a^2 \phi_d^2 \tag{4}$$

where ξ is a numerical factor, σ is the surface tension.

Units Verification:

– *LHS:*

$$\frac{F_{\text{int}}}{N} \quad (\text{Units: } \frac{\text{J}}{1} = \text{J})$$

– *RHS:*

$$4\pi\xi\sigma a^2 \phi_d^2 \quad (\text{Units: } \text{J/m}^2 \times \text{m}^2 = \text{J})$$

The units on both sides of the equation (4) are consistent, with both sides having units of energy (J).

These three energy terms are incorporated into a total free energy expression as follows:

$$F_{\text{tot}}(\phi, \phi_d) = F_{\text{ent}}(\phi, \phi_d) + F_{\text{elec}}(\phi, \phi_d) + F_{\text{int}}(\phi_d), \tag{5}$$

To satisfy the near-equilibrium condition dictated by the second law of thermodynamics, the deformation volume fraction, ϕ_d, evolves based on the minimization of the total free energy, F_{tot}. At a given droplet volume fraction, ϕ, and strain rate, $\gamma = 0$, the system reaches a steady-state configuration when ϕ_d assumes its equilibrium value, denoted as ϕ_d^*. This equilibrium value, ϕ_d^*, is determined by the condition:

$$\left.\frac{\partial F_{\text{tot}}}{\partial \phi_d}\right|_{\phi_d = \phi_d^*} = 0. \tag{6}$$

The dependence of ϕ_d^* on ϕ reflects the natural progression of the system to a state where entropic, electrostatic and interfacial forces are balanced. In this state, ϕ_d^* captures the volume fraction of deformation that minimizes the total free energy, ensuring thermodynamic stability under the given conditions. Thus, ϕ_d can be regarded as a dynamic parameter, while ϕ_d^* represents the equilibrium counterpart parameter in the minimized energy configuration.

Refer to the original paper, in order to obtain the ϕ_d that could minimize the total free energy, the droplet volume fraction ϕ ranges from 0.45 to 0.85 and set the initial shear strain $\gamma = 0$ in the simulations. To find the optimal value of ϕ_d^*, we define a function `find_min_phi_d` in Python. This function minimizes the total free energy F_{tot} with respect to ϕ_d for a given volume fraction ϕ and shear strain γ. We use the `minimize_scalar` function from the `scipy.optimize` module to find the value of ϕ_d^* that minimizes F_{tot}. The graph of ϕ_d^* as a function of ϕ with a logarithmic scale on the y-axis when $\gamma = 0$ is shown below:

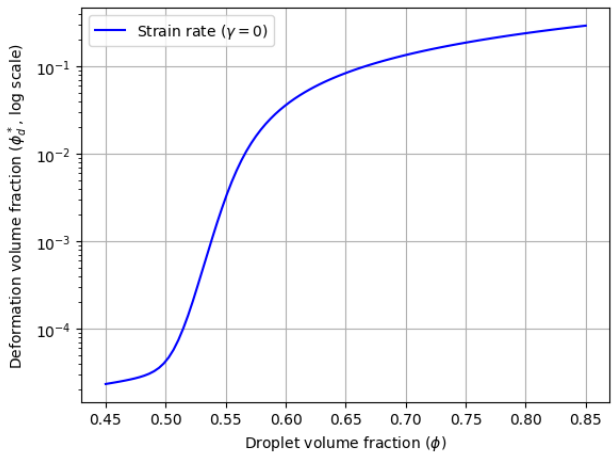

Figure 1: Deformation volume fraction (ϕ_d^*, log scale) vs droplet volume fraction (ϕ) for strain rate ($\gamma = 0$)

In our approach, we chose to find ϕ_d^* by directly minimizing the total free energy F_{tot} with respect to ϕ_d^*, instead of using the condition (6). Our decision was based on practical experiments in Python and Julia using different programming languages and optimization functions. We found

that solving ϕ_d^* using the derivative method hardly leads to a change in ϕ_d^* when ϕ is relatively small, and the results are almost identical. This lack of change in ϕ_d^* creates problems in later G_p' or Π calculations due to the minimization of the dependence on ϕ_d^*. By choosing to minimize $F_{texttot}$ directly, we can obtain a more stable and variable value of ϕ_d^*, which will lead to more accurate and consistent results for subsequent calculations.

Typo

The deformation volume fraction ϕ_d depends on both ϕ and γ, i.e., $\phi_d = \phi_d(\phi, \gamma)$. As a result, the derivative of F_{tot}/N with respect to ϕ or γ includes the implicit dependence of ϕ_d^* on these variables. Specifically, $\frac{\partial(F_{\text{tot}}/N)}{\partial\phi}$, accounts for the variation of ϕ_d^*, which minimizes F_{tot}/N, as a function of ϕ and γ. Ignoring this dependence may lead to the incorrect assumption that the free energy is constant with respect to ϕ or γ, which is not the case. To illustrate this relationship, we conducted two analyses. First, we examined ϕ_d^* as a function of γ for a fixed $\phi = 0.55$, providing insights into how the strain rate influences the deformation volume fraction. Second, we analyzed ϕ_d^* across a range of ϕ values from 0.45 to 0.85 and γ values from 0 to 0.01, revealing the combined effects of droplet volume fraction and strain rate on ϕ_d^*. The resulting plots highlight the dependence of ϕ_d^* on both ϕ and γ.

Are you sure this is a log scale?

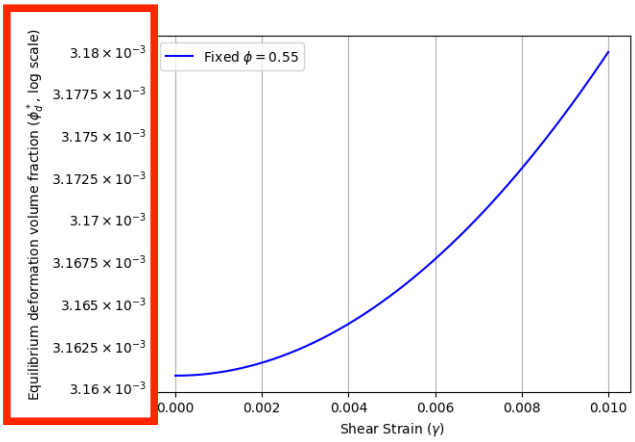

Figure 2: Equilibrium deformation volume fraction (ϕ_d^*) as a function of strain rate (γ) for fixed droplet volume fraction ($\phi = 0.55$).

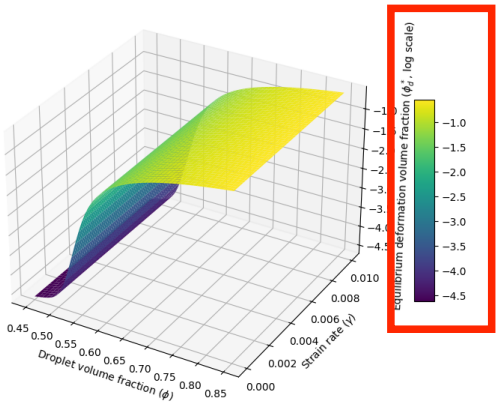

Why more variation (three orders of magnitude) than in previous case?

Figure 3: Equilibrium deformation volume fraction (ϕ_d^*) as a function of droplet volume fraction (ϕ) and strain rate (γ)

After obtaining the optimal value of ϕ_d through direct minimization, we substitute this ϕ_d back into the original equations (1), (2), and (4) for the respective terms F_{tot}, F_{int}, F_{ent}, and F_{elec}. This allows us to compute each component of the free energy based on the optimized ϕ_d.
The resulting plots for each free energy term per droplet are shown in comparison with the corresponding figures from the original paper. Below, we present a side-by-side comparison of our computed results (left) and the original results from the paper (right). Note that the vertical axis represents the free energy normalized by k_BT (i.e., in units of k_BT), and the values are plotted on a log scale.

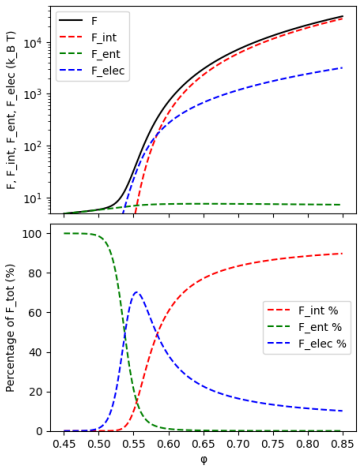

Figure 4: Our results

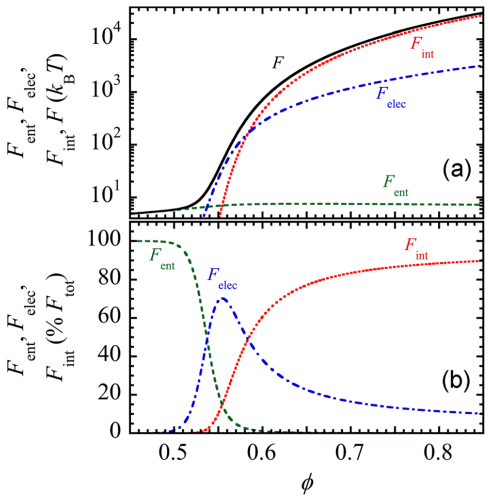

Figure 5: Original results from the paper

2 The Osmotic Pressure

To calculate the osmotic pressure Π, we use the formula in the paper:

$$\Pi = \left[\frac{\phi^2}{NV_{\text{drop}}}\right]\left[\frac{\partial F_{\text{tot}}}{\partial \phi}\right]_{\phi_d=\phi_d^*,\gamma=0} = \left[\frac{\phi^2}{V_{\text{drop}}}\right]\left[\frac{\partial (F_{\text{tot}}/N)}{\partial \phi}\right]_{\phi_d=\phi_d^*,\gamma=0} \tag{7}$$

Here, V_{drop} represents the volume of a single droplet. The osmotic pressure Π is thus dependent on the derivative of the total free energy per droplet F_{tot}/N with respect to ϕ, evaluated at the optimal deformation volume fraction ϕ_d^* and $\gamma = 0$.

To compute each component of Π (including the total and individual contributions from F_{int}, F_{ent}, and F_{elec}), we use the optimal value ϕ_d^* obtained as before, and calculate the first-order derivatives of each energy component with respect to ϕ by `np.gradient` function from `NumPy` library, under the values of ϕ vary between 0.45 and 0.85, and γ values range from 0 to 0.01. This function is used to compute the numerical gradient (approximate derivative) of an array and it is particularly useful for estimating the rate of change in a dataset when an analytical derivative is not available. Using these derivatives, we can then calculate the osmotic pressures for each component according to the formula (7). The resulting plots for each term per droplet are shown in comparison with the corresponding figures from the original paper. Below, we present a side-by-side comparison of our computed results (left) and the original results from the paper (right).

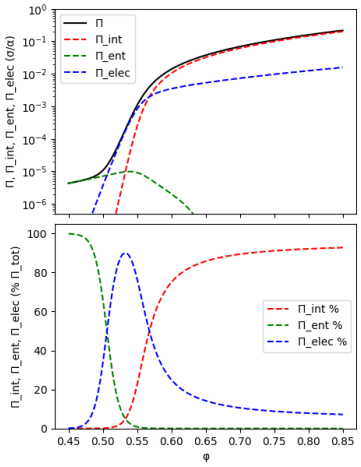

Figure 6: Our results

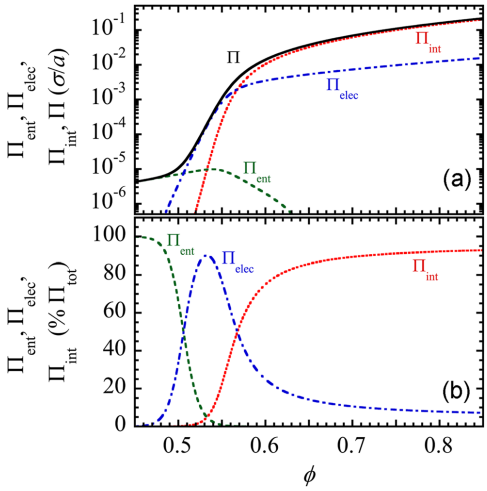

Figure 7: Original results from the paper

3 The Plateau Elastic Shear Moduli

To calculate the plateau elastic shear moduli G_p', we use the formula in the paper:

$$
\begin{aligned}
G_p' &= \left[\frac{\phi}{N V_{\text{drop}}}\right]\left[\frac{\partial^2 F_{\text{tot}}}{\partial \gamma^2}\right]_{\phi_d=\phi_d^*,\gamma=0} \\
&= \left(\frac{\phi}{V_{\text{drop}}}\right)\cdot\left(\frac{\partial^2\left(\frac{F_{\text{tot}}}{N}\right)}{\partial \gamma^2}\right)_{\phi_d=\phi_d^*,\gamma=0}.
\end{aligned} \tag{8}
$$

Using the values of ϕ vary between 0.45 and 0.85, and γ values range from 0 to 0.01, we could get the optimal deformation volume fraction ϕ_d for each combination. After obtaining F_{tot} and its components for different γ values at each ϕ, we use cubic spline interpolation to smooth these values. This interpolation creates a continuous function, allowing us to compute second derivatives with respect to γ. Using the cubic splines, we calculate the second derivative of F_{tot} and each component (F_{int}, F_{ent}, F_{elec}) with respect to γ. We use `spline_tot.derivative(2)` to obtain the second derivative of each spline function. The second derivative is evaluated at $\gamma = 0$ by selecting the value at the first index of the γ array as a close approximation. Using the formula (8) we calculate G_p' for the total free energy and each component.

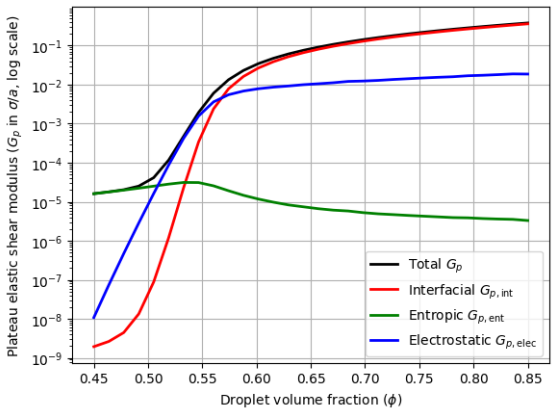

Figure 8: Plateau elastic shear modulus (G'_p) and its components as functions of ϕ for $num = 30$. The vertical axis is in units of σ/a (log scale).

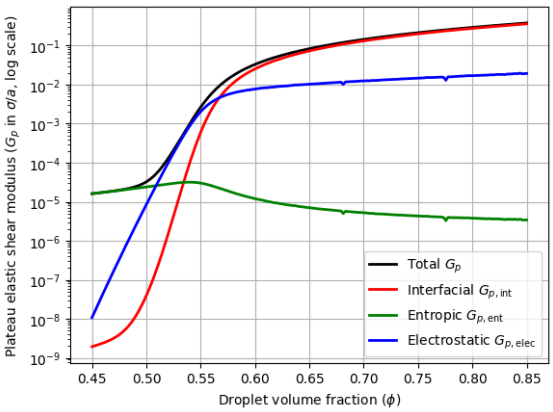

Figure 9: Plateau elastic shear modulus (G'_p) and its components as functions of ϕ for $num = 200$. The vertical axis is in units of σ/a (log scale).

The results are shown in Figure 8 and 9. To analyze the plateau elastic shear modulus (G'_p) and its relative contributions, we generated two sets of plots with different numbers of sampling points for ϕ. For the first plot, we divided the range of ϕ ($0.45 \leq \phi \leq 0.85$) into 30 values. Due to the lower resolution, the plot appears more scattered, leading to less continuity in the relative contributions of the different components ($G'_{p,\text{int}}, G'_{p,\text{ent}}, G'_{p,\text{elec}}$). In contrast, the second plot divides the same range of ϕ into 200 values, providing a much smoother representation of the relative contributions. Upon closer inspection, two noticeable singularities are observed for the electrostatic component ($G'_{p,\text{elec}}$) and the entropic component ($G'_{p,\text{ent}}$) at $\phi = 0.6811$ (corresponding to `phi_vals[115]`) and $\phi = 0.7756$ (corresponding to `phi_vals[162]`), respectively. Both plots use a vertical axis scaled in logarithmic units of σ/a to clearly display the wide range of values for G'_p and its components. The components analyzed include the total plateau elastic shear modulus (G'_p), the interfacial contribution ($G_{p,\text{int}}$), the entropic contribution ($G_{p,\text{ent}}$), and the electrostatic contribution ($G_{p,\text{elec}}$).

Upon analyzing the cubic spline interpolation of F, we find that it appears quite smooth. However, the first and second derivatives show two distinct singularities. The exact cause of these singularities remains unclear, and as such, we have not yet determined an approach to address them. To enhance the visual smoothness of the plots, we apply a Gaussian filter with $\sigma = 3$ using `gaussian_filter1d` to smooth the function. The resulting plots for each term are shown in comparison with the corresponding figures from the original paper. Below, we present a side-by-side comparison of our computed results (left) and the original results from the paper (right).

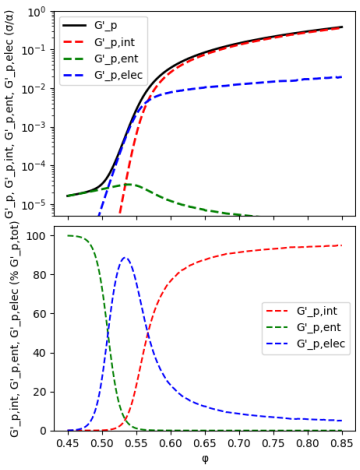

Figure 10: Our results (after smoothed)

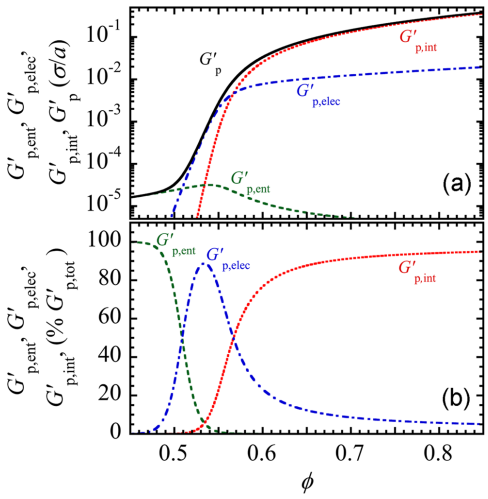

Figure 11: Original results from the paper

4 Improvements for experimental validation

4.1 Consider T as a variable

4.1.1 The Debye screening length

The Debye screening length, denoted as λ_{D}, is a key parameter in understanding electrostatic interactions in solutions. It can be calculated using the formula:

$$\lambda_{\mathrm{D}} = \left[\frac{\varepsilon_{\mathrm{r}}\varepsilon_0 k_{\mathrm{B}} T}{2e^2 I}\right]^{1/2}, \tag{9}$$

as described by Russel et al. [3]. In this equation, e is the elementary charge, approximately equal to 1.602×10^{-19}, and I is the ionic strength of the solution. For our sodium dodecyl sulfate (SDS) solution, the ionic strength is approximately $I \approx 8.2$ mM. This value corresponds to the known critical micelle concentration (CMC) of SDS (Scheffold et al. [4]; Umlong and Ismail [5]). Plugging these values into the formula (9) under temperature $T = 298K$, gives us a Debye length of about $\lambda_{\mathrm{D}} = 3.357343068814714 \times 10^{-09}\ m \approx 3.4\ nm$.

4.1.2 The surface potential

The surface potential ψ_0 is another important variable. In the paper, $|\psi_0| = 270$ mV is determined by optimizing the global fit of the EEI model,and this value is close to the estimate from Grahame's equation:

$$\psi_0 = \left[\frac{2k_{\mathrm{B}}T}{ze}\right] \sinh^{-1}\left[\frac{\sigma_{\mathrm{e}}}{(8c_0\varepsilon_{\mathrm{r}}\varepsilon_0 RT)^{1/2}}\right], \tag{10}$$

which is based on Gouy-Chapman theory (Russel et al. [3]). In this equation, σ_{e} is the surface charge density, c_0 is the bulk molar concentration of the counterions, R is the gas constant, and $z = 1$ for monovalent ions like those from dissociated SDS. For our calculations, we used a measured value of the surface charge density $\sigma_{\mathrm{e}} \approx 2\,e/\mathrm{nm}^2$. This value is reported for the adsorbed surface

density of dodecyl sulfate anions (DS^-) at the interface of decane and water when $c_0 = [SDS] = 10$ mM (Cockbain [1]). Plugging these values into the formula (10) under temperature $T = 298K$, gives us a surface potential of about $\psi_0 = 0.2053899583186848V \approx 210\ mV$.

4.1.3 Effect of Temperature T on Elastic Modulus G'_p

By treating T as a variable, we can analyze how G'_p changes with temperature. For example, at $T = 298$ K, we could compute G'_p using the similar method as before, the results are as follows:

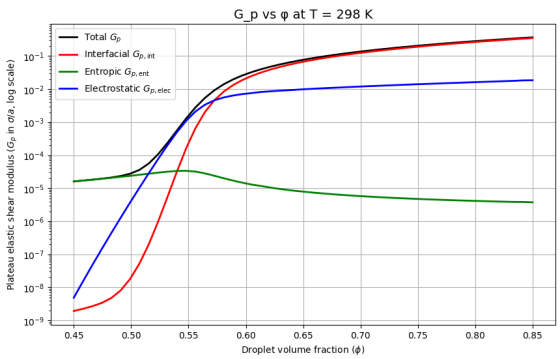

Figure 12: Plateau elastic shear modulus (G'_p) and its components as functions of ϕ for $num = 50$. The vertical axis is in units of σ/a (log scale).

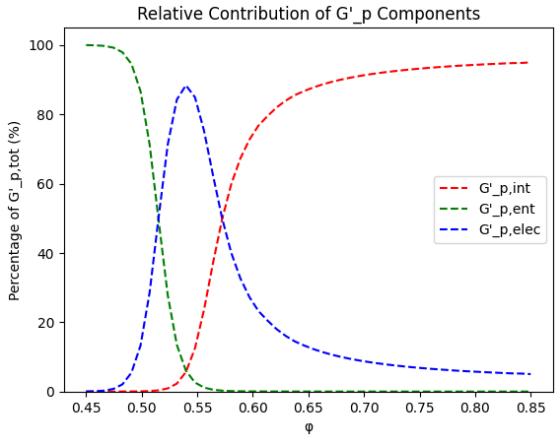

Figure 13: Percent relative contributions of $G'_{\text{p, ent}}$, $G'_{\text{p,elec}}$, and $G'_{\text{p,int}}$ to the total G'_{p}

4.2 Comparison between experimental data and model results.

	Mayo 1	Mayo 2	Mayo 3	Mayo 4	Mayo 5
Oil volume (%)	75.0	70.0	75.0	70.0	65.0
Droplet size (micron)	5.1	8.0	8.0	16.0	11.9
Ionic strength (mM)	5.0	5.0	1000.0	10.0	10.0
Surface tension (mN/m)	6.6	6.6	8.0	6.0	6.0
Zeta potential (mV)	40.0	-40.0	0.5	-15.0	-15.0
Experimental - Plateau elastic modulus (Pa)	750.0	241.0	1000.0	188.0	56.0
Model - Plateau elastic modulus (Pa)	335.0	106.4	239.1	45.0	7.3

Table 1: Comparison between experimental data and model results of different mayonnaise samples.

In reviewing the comparison between the experimental data and the model results shown in Table 1, we observe that the predicted plateau elastic modulus values from the model are consistently lower than the experimental measurements for all mayonnaise samples. This indicates that the model does not fully capture all the factors affecting the rheological properties of the mayonnaise emulsions.

References

[1] EG Cockbain. The adsorption of sodium dodecyl sulphate at the oil-water interface and application of the gibbs equation. *Transactions of the Faraday Society*, 50:874–881, 1954.

[2] Ha Seong Kim, Frank Scheffold, and Thomas G Mason. Entropic, electrostatic, and interfacial regimes in concentrated disordered ionic emulsions. *Rheologica Acta*, 55:683–697, 2016.

[3] William Bailey Russel, WB Russel, Dudley A Saville, and William Raymond Schowalter. *Colloidal dispersions*. Cambridge university press, 1991.

[4] Frank Scheffold, James N Wilking, Jakub Haberko, Frédéric Cardinaux, and Thomas G Mason. The jamming elasticity of emulsions stabilized by ionic surfactants. *Soft Matter*, 10(28):5040–5044, 2014.

[5] IM Umlong and K Ismail. Micellization behaviour of sodium dodecyl sulfate in different electrolyte media. *Colloids and Surfaces A: Physicochemical and Engineering Aspects*, 299(1-3): 8–14, 2007.